

of volumetric flow rates with an accuracy of  $\pm 18\%$  when compared to previously reported data.<sup>2,4,6</sup>

### References

- <sup>1</sup>Pond, R., U.S. Patent no. 2,825,108, 1959.
- <sup>2</sup>Kavesh, S., "Principles of Fabrication," *Metallic Glasses*, American Society for Metals, Metals Park, OH, 1978, pp. 36–73.
- <sup>3</sup>Hillmann, H., and Hilzinger, H. R., "On the Formation of Amorphous Ribbons by the Melt Spin Technique," *Proceedings of the 3rd International Conference on Rapidly Quenched Metals* (Brighton, England, UK), Vol. 1, Metals Society, London, Vol. 22, No. 9, 1978, p. 446.
- <sup>4</sup>Liebermann, H. H., "The Dependence of the Geometry of Glassy Alloy Ribbons on the Chill-Block Melt-Spinning Process Parameters," *Materials Science and Engineering*, Vol. 43, No. 3, 1980, pp. 203–210.
- <sup>5</sup>Vincent, J. H., Herbertson, J. G., and Davies, H. A., "The Process Physics of Melt Spinning and Planar Flow Casting," *Proceedings of the 4th International Conference on Rapidly Quenched Metals*, Vol. 1, Japan Inst. of Metals, Sendai, Japan, 1981, 1982, p. 77.
- <sup>6</sup>Pavuna, D., "Production of Metallic-Glass Ribbons by the Chill-Block Melt-Spinning Technique in Stabilized Laboratory Conditions," *Journal of Materials Science*, Vol. 16, No. 9, 1981, pp. 2419–2433.
- <sup>7</sup>Anestiev, L. A., and Russev, K. A., "On the Fluid-Dynamics of the Formation of Thin Metal Ribbons by Rapid Quenching from the Melt," *Materials Science and Engineering*, Vol. 95, Nov. 1987, pp. 281–286.
- <sup>8</sup>Anestiev, L. A., "An Analysis of Heat and Mass-Transfer and Ribbon Formation by Rapid Quenching from the Melt," *Materials Science and Engineering A—Structural Materials Properties Microstructure and Processing*, Vol. 110, March 1989, pp. 131–138.
- <sup>9</sup>Anestiev, L. A., "An Analysis of the Heat and Momentum Transfer During Rapid Quenching of Some Microcrystalline Materials from the Melt," *Journal of Materials Science*, Vol. 25, No. 1A, 1990, pp. 233–240.
- <sup>10</sup>Taha, M. A., Mahallawy, N. A., and Abdelgaffar, M. F., "Geometry of Melt-Spun Ribbons," *Materials Science and Engineering A—Structural Materials Properties Microstructure and Processing*, Vol. 134, March 1991, pp. 1162–1165.

## Emittance Measurements for a Thin Liquid Sheet Flow

Amy N. Englehart\*

Cleveland State University, Cleveland, Ohio 44115

Marc W. McConley†

Massachusetts Institute of Technology,  
Cambridge, Massachusetts 02139

and

Donald L. Chubb‡

NASA Lewis Research Center, Cleveland, Ohio 44135

### Introduction

THE liquid sheet radiator (LSR) is an external flow radiator that uses a triangular-shaped flowing liquid sheet as the

Received Oct. 23, 1995; presented as Paper 96-0237 at the AIAA 34th Aerospace Sciences Meeting and Exhibit, Reno, NV, Jan. 15–18, 1996; revision received Feb. 26, 1996; accepted for publication March 4, 1996. Copyright © 1996 by the American Institute of Aeronautics and Astronautics, Inc. All rights reserved.

\*Student, Department of Electrical Engineering, 1983 E. 24th Street.

†Ph.D. Candidate, Aeronautics and Astronautics, Draper Laboratory, M/S 3-H, 555 Technology Square. Student Member AIAA.

‡Research Engineer, Photovoltaics Branch, 21000 Brookpark Road. Member AIAA.

radiating surface. It has potentially much lower mass than solid wall radiators such as pumped loop and heat pipe radiators, along with being nearly immune to micrometeoroid penetration. The LSR has an added advantage of simplicity. Surface tension causes a thin (100–300- $\mu\text{m}$ ) liquid sheet to coalesce to a point, causing the sheet flow to have a triangular shape. Such a triangular sheet is desirable since it allows for simple collection of the flow at a single point.

A major problem for all external flow radiators is the requirement that the working fluid be of very low ( $\sim 10^{-8}$  torr) vapor pressure to keep evaporative losses low. As a result, working fluids are limited to certain oils (such as used in diffusion pumps) for low temperatures (300–400 K) and liquid metals for higher temperatures.

Previous research on the LSR has been directed at understanding the fluid mechanics of thin sheet flows<sup>1,2</sup> and assessing the stability of such flows, especially with regard to the formation of holes in the sheet.<sup>3</sup> Taylor<sup>4–6</sup> studied extensively the stability of thin liquid sheets both theoretically and experimentally. He showed that thin sheets in a vacuum are stable. The latest research has been directed at determining the emittance of thin sheet flows. The emittance was calculated from spectral transmittance data for the Dow Corning 705 silicone oil. By experimentally setting up a sheet flow, the emittance was also determined as a function of measurable quantities, most importantly, the temperature drop between the top of the sheet and the temperature at the coalescence point of the sheet. Temperature fluctuations upstream of the liquid sheet were a potential problem in the analysis and were investigated.

### Analysis and Results

#### Sheet Emittance from Transmittance Data

The following expression is given for the spectral emittance  $\epsilon_\lambda$  of an infinite sheet,<sup>1</sup>

$$\epsilon_\lambda = 1 - t_\lambda = 1 - 2E_3(\alpha_\lambda \tau) \quad (1)$$

where  $t_\lambda$  is the spectral transmittance,  $\alpha_\lambda$  is the extinction coefficient,  $\tau$  is the thickness of the sheet, and  $E_3(x)$  is the exponential integral of order three. In obtaining Eq. (1) reflection at the vacuum, sheet interface has been neglected. Including all reflection results in a more complex expression for the emittance.<sup>7</sup> The major correction to Eq. (1) is that it should be multiplied by  $(1 - R)$ , where  $R$  is the reflectance at the vacuum-sheet interface. Using an index of refraction,  $n = 1.58$ ,<sup>8</sup> results in a normal reflectance of  $R = (n - 1)^2 / (n + 1)^2 = 0.05$ . Therefore, to first order, the inclusion of reflectance results in a less than 10% correction to Eq. (1). The total hemispherical emittance is defined as follows<sup>9</sup>:

$$\epsilon = \frac{\int_0^\infty \epsilon_\lambda e_{\lambda b}(\lambda, T) d\lambda}{\sigma_{sb} T^4} \quad (2)$$

where  $e_{\lambda b}$  is the blackbody hemispherical spectral emissive power,  $T$  is the temperature,  $\lambda$  is the wavelength, and  $\sigma_{sb}$  is the Stefan-Boltzmann constant ( $5.67 \times 10^{-8} \text{ W/m}^2 \text{ K}^4$ ).

From the measured spectral transmission of the oil  $t_\lambda$ , the extinction coefficient  $\alpha_\lambda$  is calculated as given in Ref. 10. The total emittance  $\epsilon$  is then calculated for any thickness  $\tau$ , and any temperature  $T$ , using Eqs. (1) and (2). Transmittance data were taken for a sample of the Dow Corning 705 silicone oil with a Fourier transform infrared (FTIR) spectrophotometer. From this transmittance data, the extinction coefficient was determined,<sup>10</sup> and the extinction coefficient is plotted as a function of wavelength in Fig. 1. A further advantage of Dow Corning 705 silicone oil is the extinction coefficient's maximum around 9–10  $\mu\text{m}$ . For 300–400 K, the blackbody hemispherical emissive power is a maximum at 8–10  $\mu\text{m}$ . Because

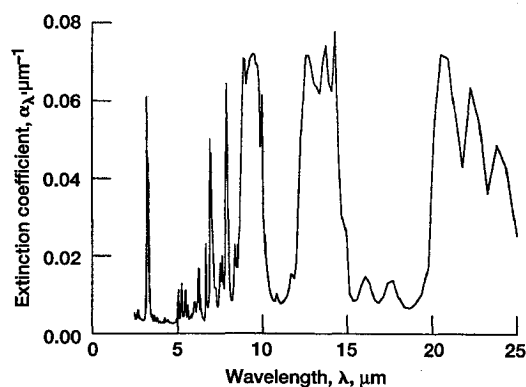


Fig. 1 Extinction coefficient for Dow Corning 705 silicone oil.

of this overlapping of maxima, the total hemispherical emittance will be large for the 300–400 K temperature region, which is a typical bottom temperature in a space-heat engine cycle. For the temperature range (300–400 K) where the silicone oils can be used,  $\epsilon_{\lambda b}$  is negligible for  $\lambda < 2.5 \mu\text{m}$  and also for  $\lambda > 70 \mu\text{m}$ . Because of this the integration in Eq. (2) was carried out for the wavelength region  $2.5 < \lambda < 70 \mu\text{m}$ .

#### Sheet Emittance from Measured Temperature Drop

The working fluid flows in the  $z$  direction from a slit of prescribed width  $W$  and thickness  $\tau$ . It coalesces to a point at  $z = L$  to form a triangular sheet of liquid of length  $L$  with the planform area of the sheet acting as a radiating surface. When surrounded by a sink temperature  $T_\infty$ , lower than the initial fluid temperature, the fluid temperature decreases as a function of the vertical position  $z$ , until reaching the coalescence point.

A number of simplifying assumptions can be made. Although the sheet thickness decreases with distance from the slit because of gravity, the effect may be neglected because the Froude number (the ratio of the kinetic energy to gravitational potential energy) for this experiment is high enough that gravitational effects on the sheet geometry can be neglected. Also because of the large Froude number, the sheet shape is exactly triangular.<sup>2</sup> If heat transfer caused by conduction and convection is neglected (this is reasonable provided a sufficient vacuum is maintained), then in the steady state, the radiated power must balance the enthalpy change

$$P_{\text{rad}} = 2\sigma_{\text{sb}} \int_A \epsilon(T^4 - T_\infty^4) dA = \rho Q C_p (T_1 - T_2) \quad (3)$$

where  $T$  is the temperature of the sheet,  $A$  is the sheet area,  $\epsilon$  is the total hemispherical emittance,  $\rho$  is the density of the fluid,  $C_p$  is the specific heat,  $Q$  is the volumetric flow rate,  $T_1$  is the temperature of the oil at the top of the sheet, and  $T_2$  is the temperature at the coalescence point. The factor of 2 arises because both sides of the sheet radiate. The background in the experiment is a black painted surface. It is assumed to behave as a blackbody with  $\epsilon_\infty = 1$  and a constant temperature. It is assumed that the emittance and sink temperature are constant for the sheet area and that  $T$  varies only in the  $z$ -direction. In Ref. 10, the solution to the steady-state energy equation is carried out to determine  $T(z)$ , which can then be used to do the integration in Eq. (3). However, since the temperature drop  $\Delta T = T_1 - T_2$  is only a few tenths of a degree in our experiment, the approximation  $T = T_1$  may be made in Eq. (3) with a percent deviation of less than 1%.<sup>10</sup> This gives the following:

$$\epsilon = \frac{\rho C_p Q \Delta T}{\sigma_{\text{sb}} W L (T_1^4 - T_\infty^4)} \quad (4)$$

The emittance is calculated directly from Eq. (4) provided measurements are available for the three temperatures  $T_1$ ,  $T_2$ , and  $T_\infty$ ; the flow rate  $Q$ ; and the sheet length  $L$ . The specific heat  $C_p$  and the density  $\rho$  were measured as functions of temperature at NASA Lewis Research Center.

The test facility that was used consists of a 30-cm-i.d. stainless-steel pipe 3.5 m long. The axis of the pipe was aligned with the gravity field ( $z$  direction). Vacuum conditions existed within the pipe with the pressure about 0.02–0.04 torr. At these conditions, aerodynamic drag on the sheet flow, as well as heat transfer from conduction and convection, was negligible. Dow Corning 705 silicone oil was pumped up to a 10 gal plenum above the slit. Within the plenum, vibrations and temperature fluctuations were effectively damped out. The fluid temperature was maintained at 373 K. Four different slit plate sizes were tested:  $\tau = 100 \mu\text{m} \times W = 12.5 \text{ cm}$ ,  $\tau = 150 \mu\text{m} \times W = 23.5 \text{ cm}$ ,  $\tau = 200 \mu\text{m} \times W = 23.5 \text{ cm}$ , and  $\tau = 300 \mu\text{m} \times W = 18.75 \text{ cm}$ .

With these conditions, the temperature drop is very small, around 0.3 K. For this reason, carefully calibrated ultrastable thermistors were used to measure  $T_1$  and  $T_2$ . Other techniques, such as optical techniques, would be unable to give the temperature resolution needed. The thermistors are responsive to 0.01 K temperature changes. The upper thermistor was located right above the slit in the plenum. The lower thermistor was located on an actuator platform on which the thermistor swung around horizontally. The platform traveled vertically and the thermistor was positioned directly in the coalescence point to get the full temperature drop  $T_1 - T_2$ . Since the vessel was enclosed, the actuator had video camera and light to visually position the thermistor in the flow.

A coolant continuously circulated between a baffle and the vessel wall to maintain the sink temperature at a constant 300 K and thermocouples measured the sink temperature. To measure  $Q$  a calibration done at NASA Lewis Research Center of the pressure drop across a calibrated orifice in the oil supply line was used to measure  $Q$  (Ref. 10). To measure  $L$  the actuator probe's vertical position was recorded when the lower thermistor was positioned in the coalescence point. With these measured values, the emittance was calculated.

An experimental investigation of temperature fluctuations was also carried out. The thermistors response time is 1.5 s, thus, experiments were conducted where  $T_1$  was measured at 1.5-s intervals. The average temperature change in this interval was found to be 0.031 K and the largest temperature change was found to be 0.054 K. Fluctuations of 0.05 K or greater occurred 17% of the time. 0.05 K is large for our purposes, however, if the period of the fluctuations is much greater than the flow time (the time it takes a particle to traverse the sheet or  $L/w_0$  and  $w_0$  is the velocity in the  $z$  direction), then the temperature fluctuation's effect on  $\Delta T$  will not be significant. The flow time was calculated and found to be 0.081 s for the 100- $\mu\text{m}$  sheet, 0.185 for the 150- $\mu\text{m}$  sheet, 0.214 s for the 200- $\mu\text{m}$  sheet, and 0.209 s for the 300- $\mu\text{m}$  sheet. These flow times are not small enough to ignore the fluctuations upstream of the slit plate. Thus, to eliminate the fluctuations as many precautions as were available were taken. The facility is insulated everywhere and the only possible source of temperature fluctuations introduced are from the heaters. To eliminate any heater fluctuations, the heaters were turned off during the time the data were taken.

The resulting experimental emittance using Eq. (4) along with the theoretical emittance using Eq. (1) is shown in Fig. 2. The emittance of the oil in the 300–400 K region proved to be quite high. The experimental emittance of the sheet is between 0.74–0.85, depending on the sheet thickness and oil temperature. The percent deviation for the experimental emittance is 6.8% at 100  $\mu\text{m}$ , 5.6% at 150  $\mu\text{m}$ , 2.4% at 200  $\mu\text{m}$ , and 5.0% at 300  $\mu\text{m}$ . The emittance calculated from the transmittance data agreed closely with the experimental values. The experimental values were slightly less than the theoretical val-

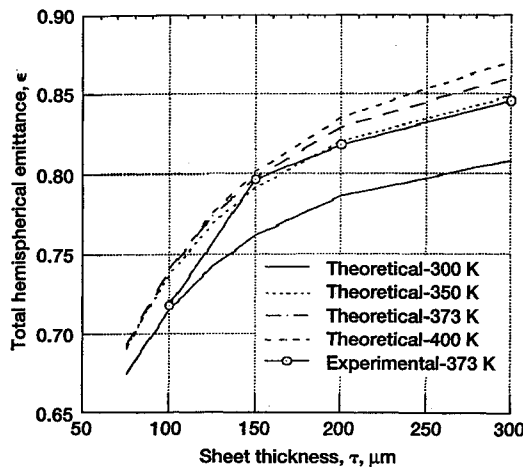


Fig. 2 Comparison of theoretical and experimental total hemispherical emittance for Dow Corning 705 oil.

ues for all sheet thicknesses. As shown in Fig. 2, the emittance increases with an increase in temperature and an increase in sheet thickness. As the temperature increases past 400 K, the blackbody hemispherical spectral power is a maximum at wavelengths shorter than 9–10  $\mu\text{m}$  where spectral emittance is a maximum. Thus, the overall hemispherical emittance will begin to decrease as the temperature increases beyond 400 K. As the sheet thickness is increased, the emittance will level off and reach a constant value.

### Conclusion

The emittance of a thin liquid sheet flow of Dow Corning 705 oil was determined by two methods. From the analysis and results, several points can be made. It is evident that the Dow Corning 705 liquid sheet has a strong potential of functioning well as a radiator. The experimental emittance and the calculated emittance show high values averaging from 0.74 to 0.85. Because reflectance was neglected in Eq. (1), the calculated emittance has an error of approximately 5%. Experimentally, it was difficult to determine if the temperature fluctuations were insignificant, but efforts were made to eliminate any fluctuations. Thus far, research on the liquid sheet indicates it is an excellent candidate for a low mass space radiator.

### References

- Chubb, D. L., and White, K. A., III, "Liquid Sheet Radiator," AIAA Paper 87-1525, 1987; also NASA TM 89841, June 1987.
- Chubb, D. L., Calfo, F. D., McConley, M. W., McMaster, M. S., and Afijeh, A. A., "The Geometry of Thin Liquid Sheet Flows," *AIAA Journal*, Vol. 32, No. 6, 1993, pp. 1325–1328.
- Chubb, D. L., Calfo, F. D., and McMaster, M. S., "Current Status of Liquid Sheet Radiator Research," NASA TM 105764, Feb. 1993.
- Taylor, G. I., "The Dynamics of Thin Sheets of Fluid, I. Water Bells," *Proceedings of the Royal Society of London*, Vol. A253, Dec. 1959, pp. 289–295.
- Taylor, G. I., "The Dynamics of Thin Sheets of Fluid, II. Waves on Fluid Sheets," *Proceedings of the Royal Society of London*, Vol. A253, Dec. 1959, pp. 296–312.
- Taylor, G. I., "The Dynamics of Thin Sheets of Fluid, III. Disintegration of Fluid Sheets," *Proceedings of the Royal Society of London*, Vol. A253, Dec. 1959, pp. 313–321.
- Chubb, D. L., Lowe, R. A., and Good, B. S., "Emittance Theory for Thin Film Selective Emitter," *The 1st NREL Conference on TPV Generation of Electricity*, American Inst. of Physics ACP 321, 1994, p. 235.
- Dow Corning, Dow Corning Sales Specification, South Saginaw Road, Midland, MI.
- Siegel, R., and Howell, J. R., *Thermal Radiation Heat Transfer*, 2nd ed., Hemisphere, Washington, DC, 1981, p. 52.
- Englehart, A. N., Chubb, D. L., and McConley, M. W., "Theoretical and Experimental Emittance Measurements for a Thin Liquid Sheet Flow," NASA TM 107026, Jan. 1996.

## Comparison of Numerical Quadrature Schemes Applied in the Method of Discrete Transfer

Flemming M. B. Andersen\*  
Technical University of Denmark,  
DK-2800 Lyngby, Denmark

### Introduction

**R**ADIATION heat transfer modeling is complicated by the larger number of independent variables: 1) three space coordinates describing the location, 2) two angles describing the direction, and 3) sometimes several wavelength intervals. In some applications, where the changes are fast compared to the propagation time within the geometry of the thermal radiation, the time is an independent variable. The high number of independent variables makes the solution strategy very important to obtain fast and accurate solutions of the radiative heat transfer problem.

In the method of discrete transfer, the irradiation to wall zones is calculated by a numerical quadrature that is close to the so-called midpoint method.<sup>1,2</sup> Although the method is very successful, other numerical quadrature schemes should be considered for possible use to reduce the calculation costs for a given numerical accuracy, or for the same computational costs, to obtain a more accurate result; this is the theme of this Note.

The geometry chosen is an infinitely long, circular cylinder with cold, black boundaries filled with an absorbing, emitting gas with constant temperature and radiative properties (see Fig. 1). The irradiation to the cylindrical wall is calculated. The analyses are valid for gray gases as well as for the monochromatic cases.

Several other numerical methods are applicable within the field of thermal radiation and some excellent references are Siegel and Howell,<sup>3</sup> Viskanta,<sup>4</sup> Viskanta and Menguc,<sup>5</sup> and Viskanta and Ramadhyani.<sup>6</sup>

### Theory

The method of discrete transfer is a ray-tracing technique for solving the radiative transfer problem primarily in absorbing and emitting gas<sup>1</sup> where the irradiation  $H$  is found by numerical integration of

$$H = \int_{\phi=0}^{2\pi} \int_{\theta=0}^{\pi/2} I \cdot \cos \theta \cdot \sin \theta \cdot d\theta \cdot d\phi \quad (1)$$

$$H = \int_{\phi=0}^{2\pi} \int_{\mu=0}^1 I \cdot \mu \cdot d\mu \cdot d\phi \quad (2)$$

$$H = \int_{\phi=0}^{2\pi} \int_{\kappa=0}^{1/2} I \cdot d\kappa \cdot d\phi \quad (3)$$

where  $\theta$  is the angle from the normal of the surface to the considered direction,  $\phi$  is the azimuthal angle (see Fig. 1),  $\mu = \cos \theta$ , and  $\kappa = \frac{1}{2}\mu^2$ . The incident intensity is denoted  $I$ . Further details of the method of discrete transfer are given in Refs. 1 and 2.

The incident intensity in a given direction is

$$I = I_b \cdot [1 - \exp(-a \cdot l)] \quad (4)$$

Received Aug. 31, 1995; revision received Jan. 25, 1996; accepted for publication March 11, 1996. Copyright © 1996 by the American Institute of Aeronautics and Astronautics, Inc. All rights reserved.

\*Research Associate, Department of Energy Engineering, Building 402.